Recovery of nutrients (N-P-K) from potassium-rich sludge anaerobic digestion side-streams by integration of a hybrid sorption-membrane ultrafiltration process: use of powder reactive sorbents as nutrient carriers

Mehrez Hermassi [1,2], Cèsar Valderrama[1], Oriol Gibert [1,3], Natalia Moreno[4], Xavier Querol[4], Narjès Harrouch Batis [2], Jose Luis Cortina[1,3]

[1] Chemical Engineering Department, Universitat Politècnica de Catalunya-Barcelona TECH, Barcelona, Spain

[2] Dept. Biol. Chem. Eng., National Institute of Applied Sciences and Technology (INSAT), University of Carthage (Tunisia)

[3] CETaqua Carretera d´Esplugues 75, 08940 Cornellà de Llobregat, Spain

[4] Institute of Environmental Assessment and Water Research IDAEA, Consejo Superior de Investigaciones Científicas (CSIC) Barcelona

*Correspondence should be addressed to: Mehrez Hermassi

Departament d'Enginyeria Química, Universitat Politècnica de Catalunya, Av. Diagonal 647, 08028 Barcelona, Spain, Tel.: 93 4011818, Fax.: 93 401 58 14

Email: mehrez.harmassi@upc.edu;

Abstract

Here, an alternative nutrient (N-P-K) recovery route from potassium-rich sludge anaerobic digestion side-streams using powder reactive sorbents (PRSs) is presented. In the first step, the optimum PRS system was determined in batch experiments with mixtures of: a) a sodium zeolite (NaP1) to facilitate the NH_4^+ and K^+ sorption; b) a Ca-zeolite (CaP1) to facilitate the removal of P by formation of Ca-

phosphates (e.g., $CaHPO_4$(s)), and c) caustic magnesia containing mixtures of MgO to facilitate the formation of $Mg/NH_4/PO_4$ minerals (e.g., struvite and magnesium phosphates). Evaluation of the continuous and simultaneous N-P-K removal with mixtures of PRSs was carried out using a hybrid sorption/filtration system with ultrafiltration (UF) hollow-fibre membranes. The dosing ratios of the PRS mixtures were optimised on the basis of the equilibrium and kinetic sorption data, and a PRS dose (<2–5 g PRS/L) was selected to ensure the hydraulic performance of the system. Under such conditions, and with synthetic anaerobic side-stream removal capacities (q_t) of 220±10 mg $N\text{-}NH_4$/g, 35±5 mg $P\text{-}PO_4$/g, and 8±2 mg K/g, removal efficiencies of 32±3, 78±5, and 26±3% for ammonium, phosphate, and potassium, respectively, were obtained for the binary mixtures of NaP1/CaP1 zeolites. Contrary to the batch results, the use of tertiary mixtures of NaP1/CaP1/MgO only improved the K removal capacity and efficiency to 18±2 mg K/g and 55±4%, respectively, while the phosphate removal capacity and efficiency remained unchanged (ca. 35±3 mg $P\text{-}PO_4$/g; 80±5%) and the ammonium capacity and efficiency were reduced to 185±12 mg $N\text{-}NH_4$/g and 20±2%, respectively, due to the competing Mg^{2+} ion effect. Nutrient removal trials with real anaerobic side-streams using binary mixtures of Na/Ca zeolites showed a reduction of both the hydraulic performance and the nutrient removal ratios due to the presence of dissolved organic matter. However, constant removal ratios of N, P, and K were recorded throughout the filtration experiments. The loaded PRSs exhibited suitable nutrient release rates and bioavailability as co-substrates for soil quality improvement. Chemical analyses detected the formation of Ca/P/O and Mg/N/P/O neo-minerals; however, the mineralogical data revealed only the formation of struvite, even when no magnesium oxide was used.

Keywords: nutrient recovery; powder reactive sorbents; Na/Ca-zeolite; caustic magnesia; hybrid sorption-membrane ultrafiltration; anaerobic side-stream

1. Introduction

Environmental impact of the urban and industrial sectors is attracting increasing attention due to the production of huge volumes of wastewater with high organic and mineral loads, mainly N, P, and K (Ledda et al., 2013; Petersen et al., 2007). N and P recovery from wastewater has become critical due to the detrimental effects of continuous waste discharges to the air, soil, and water bodies environment (Kumar and Pal, 2013). Besides global environmental damage, the increasing demand for N-P-K fertilisers and the complexity of their production are also of great concern. In addition, during the last decades, the presence of anthropogenic reactive N in the environment has strongly increased and transformed the biogeochemical nitrogen cycle, resulting in major environmental effects. Similarly, the biogeochemical P cycle is in a very critical state, since phosphate rock was recently listed as a critical raw material (European Commission, 2014). Existing studies on the depletion of phosphate rock have shown contradictory results due to a lack of comprehensive knowledge about the state of the current reserves and future exploitable P resources (Taddeo et al., 2016; Van Kauwenbergh et al., 2013). However, current environmental regulations do not deal with, and hence do not restrict, the use of potassium in agricultural applications. Nevertheless, the growing concentration of K in soil has been identified as one of the causes of mineral deficiencies, immune suppression, and reproductive losses in herbivores (Masse et al., 2007). Therefore, the recovery and removal of nutrients from the main anthropogenic flows, i.e., animal manure, urban/industrial wastewater, and agricultural run-offs, is crucial in order to maintain a sustainable environmental balance and secure a renewable source of nutrients (Taddeo et al., 2016).

In general, treatment technologies remove and/or recover pure nutrient by-products from wastewater treatment plant (WWTP) streams with limited efficiency and/or partial recovery. These limitations have prompted a new approach relying on the use of low-cost inorganic-based adsorbents (e.g., clays, fly ash, and zeolites) suitable as intermediary media to transport nutrients from wastewater to

soils for direct use as fertilisers or soil conditioners (Bartzokas, 2001; Lalley et al., 2016; Onyango et al., 2007; Schoumans et al., 2015).

Typically, the recovery of N and P from wastewater has been considered in independent processes due to their chemical nature, and their simultaneous removal by sorption processes has rarely been reported. The merit of using one single material for the simultaneous removal of both ammonium and phosphate species is obvious; however, this has not yet been achieved. In general, most of the solutions proposed for such a simultaneous removal are based on the use of two types of reagents (e.g., a cation exchanger and an anion exchanger, or a cation exchanger and an inorganic reagent to precipitate phosphate anionic species (Wu et al., 2006; Zhang et al., 2007)). Recently, Na^+-zeolite (NaP1), obtained as a waste by-product from coal fly ash, and its zeolitic Ca-modified form (CaP1) were evaluated for the recovery of ammonium and phosphate as powdered activated zeolite materials (Hermassi et al., 2016b). As a consequence, the technical challenge to implement powdered reactive sorbents in WWTP streams requires solid/liquid separation techniques, including hydrocyclones or hybrid sorption/filtration processes. In this last case, the continuous progress in pressure-driven membrane processes has facilitated the integration of powder activated carbon with ultrafiltration (UF) or nanofiltration (NF) membranes (Dong et al., 2014; Wang et al., 2016).

In a previous study, powder Ca-activated zeolite (CaP1) was used as a reactive sorbent for P recovery in a hybrid sorption/filtration system using a hollow-fibre UF crossflow configuration. Hydroxyapatite is a more thermodynamically stable phase; however, P was mainly removed as brushite ($CaHPO_4$), which has a higher release potential when applied to soils than hydroxyapatite. The main hypothesis behind this phenomenon is the influence of the crystal structure in the inhibition of phase transformations (Hermassi et al., 2016a). In the present work, the concept of reactive sorbents has been extended for the simultaneous recovery of N-P-K from anaerobic side-streams generated from the digestion of sewage sludge. For this purpose, binary and tertiary mixtures of

PRSs were used. CaP1 and NaP1 zeolites (selective sorbents for N-P-K) were blended with a rich magnesium oxide material (e.g., caustic magnesia) as a source of Mg(II) ions to promote the simultaneous removal of ammonium and phosphate species by precipitation of struvite. Then, batch equilibrium and kinetic experiments were carried out to identify the optimum blends of PRSs for the simultaneous removal of N-P-K from both simulated and real anaerobic side-streams from a WWTP. Finally, three selected blends were evaluated in a hybrid sorption-membrane UF process. The loaded sorbents were finally characterised chemically and mineralogically to identify the main extraction mechanisms and the potential N-P-K bioavailability for application as soil improvers in degraded areas.

2. Materials and methods

2.1. Materials and solutions

The Na^+-zeolite NaP1 was synthesised from combustion fly ash and a 3 M NaOH solution at 125 °C, as described elsewhere (Querol et al., 2007), and the Ca^{2+}-zeolite CaP1 was prepared by a cation-exchange process as also described elsewhere (Hermassi et al., 2016b). The maximum sorption capacities of N and P for both zeolites were obtained in previous studies from the sorption isotherm experiments as follows, 109±4 mg NH_4/g, 57±3 mg P-PO_4/g for NaP1 and 123.1±9.mg NH_4/g, 203±15 mg P-PO4/g for CaP1 (You et al., 2017; Hermassi et al., 2016b).

A powder caustic magnesia sample (Magna L) from Magnesitas Navarras (Spain) with a w/w(%) chemical composition of MgO (76), CaO (11), SiO_2 (5), and fire loss (1.5) was also used.

Two different types of model anaerobic digestion side-stream water feeds were used in both batch and continuous sorption/filtration experiments. Synthetic water solutions were prepared by dissolving known amounts of NH_4Cl, K_2HPO_4, KNO_3, $NaHCO_3$, $KHCO_3$, $MgCl_2{\cdot}6H_2O$, and $CaCl_2{\cdot}2H_2O$ salts in tap water. The concentration of the main ions was fixed using the average annual composition of an

anaerobic digestion side-stream from a WWTP in El Prat (Barcelona, Spain). Samples (250 L) from the anaerobic side-stream of the sewage sludge digester were passed through a vacuum filter in order to simplify the batch and sorption/filtration experiments.

Table 1. Chemical composition (mg/L) and pH of model water feed used in both batch and continuous sorption/filtration experiments (UF_A, UF_B, and UF_C) were described in more details in Table 2.

	Na^+	NH_4^+	K^+	Mg(II)	Ca(II)	Cl^-	SO_4^{2-}	NO_3^-	HCO_3^-	P(V)	**TOC
Synthetic water feed (UF_A, UF_B) pH = 7.8±0.2	505	678	51	99	500	2384	40	1	1322	56	5.2
Anaerobic digestion side-stream (Batch and UF_C) pH = 7.8±0.2	475	665	63	92	408	1224	4	<lq*	1301	48	299.5

*lq: limit of quantification, **TOC (Total organic carbon)

2.2 N-P-K sorption: experimental methodology

2.2.1 Batch sorption kinetic experiments

Experiments to study the influence of the sorbent nature and dose on the N-P-K recovery were performed by adding known amounts of reactive sorbent mixtures (NaP1, CaP1, and MgO) to model solutions (Table 1). A given volume (25 mL) of the feed solutions was shaken in polyethylene tubes with different weighed amounts of dry CaP1, NaP1, and MgO samples using a continuous rotary mixer at room temperature (21±1 °C). Samples were withdrawn sequentially at given times to follow the sorption time-dependence of the N-P-K species. After phase separation with a 0.2-µm syringe filter, the equilibrium pH was measured using a pH electrode (Crison GLP22) and the total phosphate, ammonium, and potassium concentrations were measured.

2.2.2 Hybrid sorption-membrane UF using PRS mixtures (NaP1, CaP1, and MgO)

The UF-PRS system consisted of a clear acrylic cylinder reactor with a volume of 60 L combined with a crossflow UF module consisting of 100 hollow fibres with a molecular weight cut-off of >100000 Da. The experimental set-up is illustrated in Figure 1. The operational conditions of each experiment are listed in Table 2.

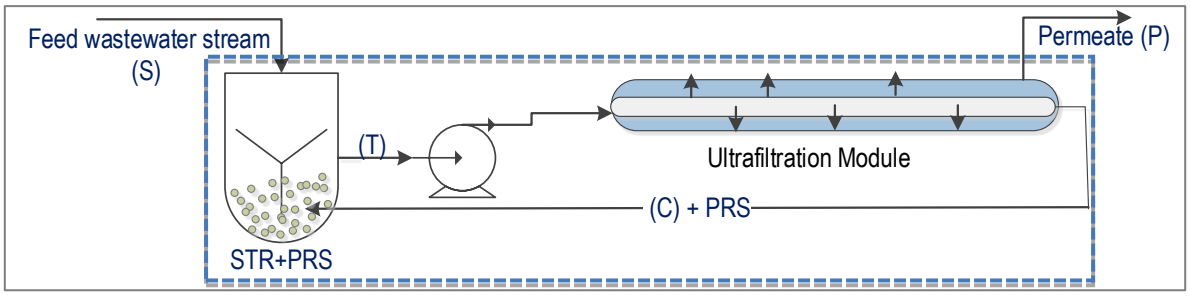

Figure 1. Schematic of the hybrid membrane sorption/UF system, including a UF hollow-fibre module, a feed wastewater stream (S), a stirred tank reactor (STR), a stream leaving the tank (T), and concentrate (C) and permeate (P) streams from the membrane module with a flow-rate of Q (m^3/s).The dashed line represents the control area used for the N-P-K mass balance.

Table 2. Operational conditions for the hybrid sorption/UF tests

Experiment	UF_A	UF_B	UF_C
Feed water	Synthetic water		Anaerobic digestion side-stream
Sorbents	CaP1 and NaP1 (32/48)	CaP1, NaP1, and MgO (32/48/20)	CaP1 and NaP1 (32/48)
pH	8±0.2	8±0.2	8±0.2
Total amount of zeolite (g/L)	2	2.5	2

Experiments were conducted as follows: 40 L of influent feed solutions and specific amounts of PRS mixtures (UF_A, UF_B, and UF_C) were added to the STR. N-P-K removal experiments were conducted as described elsewhere by Hermassi et al., 2016 (Hermassi et al., 2016a).

2.2.3 Chemical speciation and bioavailability of N-P-K in loaded PRSs

Speciation of P-N-K on the loaded PRSs was performed according to a modified four-step sequential extraction methodology (Ann et al., 2000; Hedleyet al., 1982; Moharami and Jalali, 2014). The sorbed P-K-N species were sequentially extracted using 1-g samples and 40 mL of the extraction solution, as summarised in Table S1 (Supplementary Information). The samples were mechanically shaken at 21±1 °C. Upon reaching the equilibrium (C_{eq}), the samples were centrifuged and the N-P-K content of the liquid phase was analysed. At the end of each sorption/filtration and subsequent extraction tests, the suspensions were centrifuged and the PRS samples were dried at 50–60 °C.

The bioavailability of the loaded PRS samples was evaluated using the Olsen method (Olsen, 1954). Samples (0.5 g) of loaded PRSs were mixed with 20 mL of 0.5 M $NaHCO_3$ (pH = 8±0.2) in 50-mL bottles and shaken at 21±1 °C for 24 h at a constant agitation speed (200 rpm). After phase separation with a 0.45-µm syringe filter, the equilibrium pH was measured using a pH electrode (Crison GLP22) and the samples were analysed.

2.3 Analytical methodology

The P(V) concentration was determined using the vanadomolybdophosphoric acid colorimetric method (4500-P C) in a Shimadzu UV mini-1240 UV-vis spectrophotometer. Other cations and anions were determined using a Thermo Scientific Ionic Chromatograph (Dionex ICS-1100 and ICS-1000). The bicarbonate concentration was determined potentiometrically using a 0.1 M HCl solution. The total organic carbon (TOC) content was estimated by measuring the total carbon (TC) and

inorganic carbon (IC) using a TOC-5000 instrument (Shimazdu Corporation, Japan) and then calculating the difference between them.

After completing the sorption/filtration experiments, the loaded PRS samples were examined by FSEM-EDX, and the mineral phases were identified by XRD as described elsewhere (Querol et al., 2007). Modelling of the N, P, and K precipitation processes was carried using the HYDRA-MEDUSA (Puidomènech, 2001) and Visual Minteq codes (Gray-Munro and Strong, 2013).

2.4 Evaluation of the sorption/filtration system performance: solute (N-P-K) mass balances

The performance of the hybrid membrane sorption/UF system was evaluated by estimating the removal efficiency (R–M) (%)) with Eq. 1:

$$R - M(\%) = \left(1 - \frac{C_{M-P}(t)}{C_{M-s}(t)}\right) \times 100 \quad (1)$$

where C_M represents the concentration of each N-P-K nutrient, and C_M-s(t) and C_M-p(t) represent the N-P-K concentrations in the feed and in the permeate streams, respectively, at a given time t.

The mass $M_{(P,\ N,\ and\ K)}$ sorbed on the powdered reactive sorbents (PRS(t), q(M)t (mg M/g PRS) was calculated by Eq. 2:

$$q_{M(t)} = \frac{mg(M)}{g(PRS)} = \frac{m(M)_{PRS}}{V_t * g_{PRS}} \quad (2)$$

where $m(M)_{PRS}$ is the concentration of N-P-K nutrients in the PRS per volume of solution (mg M-PRS/L)

The amount of sorbed M was calculated from the mass balance on the hybrid system schematically described in Figure 1. At time zero, the STR was filled with 40 L of an M solution with the same concentration as the feed stream (C_0). The M mass balance in the system has been properly described elsewhere by Hermassi et al., 2016 (Hermassi et al., 2016a).

196 The hydraulic performance of the UF unit was characterised by the permeation flux and membrane
197 permeability taking into account the transmembrane pressure (TMP), as described by Hermassi el
198 al., 2016 (Hermassi et al., 2016a).
199
200 **3. Results and discussion**
201 **3.1 Optimisation of PRS mixtures for N-P-K recovery using batch experiments**
202 The kinetic data for the N-P-K removal by mixtures of CaP1, NaP1, and MgO are shown in Figure 2.
203 The addition of NaP1 to CaP1 increased the ammonium removal ratio from 30% for CaP1 up to 83%
204 for a mixture of both zeolites, as shown in Figure 2a.

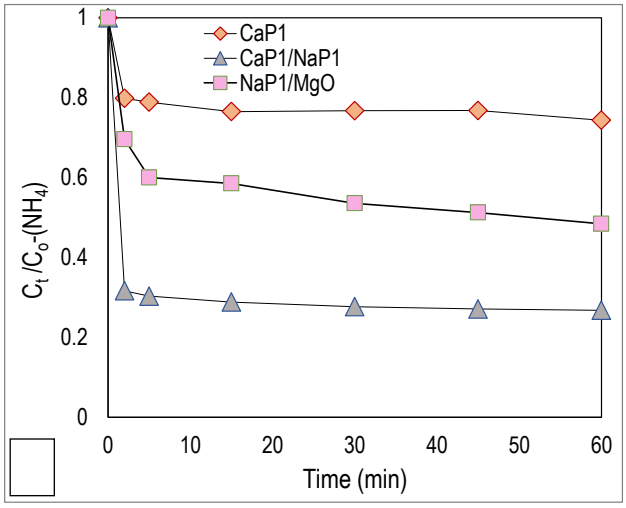
CaP1
CaP1/NaP1
NaP1/MgO
C_t/C_o-(NH_4)
Time (min)

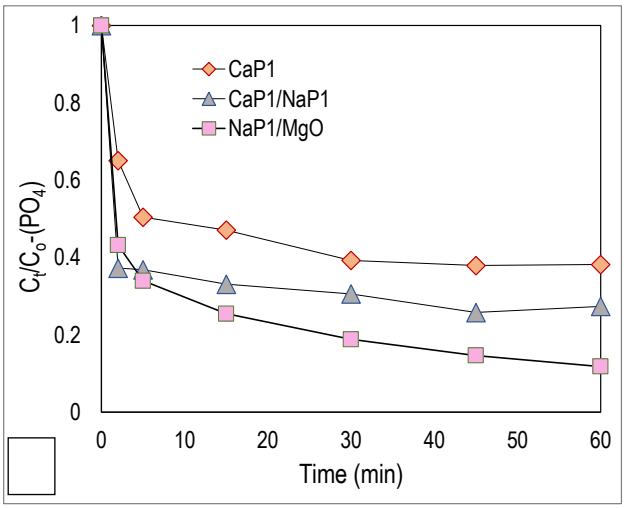
CaP1
CaP1/NaP1
NaP1/MgO
C_t/C_o-(PO_4)
Time (min)

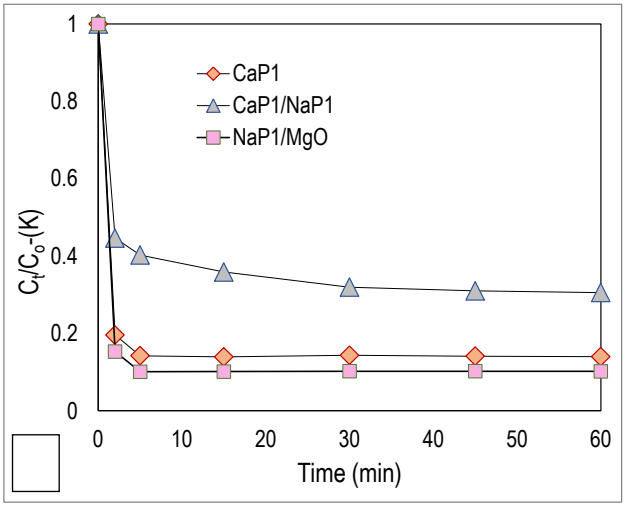
CaP1
CaP1/NaP1
NaP1/MgO
C_t/C_o-(K)
Time (min)

205

Figure 2. Evolution of a) ammonium, b) phosphate, and c) potassium sorption uptake versus time for CaP1 and mixtures of CaP1-NaP1 and NaP1-MgO in batch experiments (samples of 25 mL, constant temperature of 22±1 °C).

The ammonium and potassium cations were satisfactorily exchanged in the NaP1 and CaP1 zeolites, considering the selectivity order defined by the cation exchange constants determined as the following: K(Ca/Na) > K(NH_4/Na) > K(K/Na) > K(Mg/Na). However, the removal of phosphate was more efficient with the mixture of zeolites as, even at the lowest dose, sorption ratios above 64% were achieved (Figure 2b). Using only CaP1, a removal of 66±3% was reported by Hermassi et al. (Hermassi et al., 2016a, 2016b). CaP1 zeolite exhibits a high affinity for phosphate removal through the formation of $CaHPO_4$. Maximum recovery efficiencies for P and K (Figure 2c) were achieved when caustic magnesia MgO was added to the mixture, which reached >95% after 4 h of contact time. In fact, the pH and Mg:P molar ratio have been reported as the key factors determining the recovery efficiencies of P and K (Xu et al., 2015).

3.2 N, P, and K removal mechanisms

N-P-K removal processes are very fast, as demonstrated by the fact that the system reached equilibrium within 10 min. This phenomenon is the result of the fast exchange of Na^+ with NH_4^+ and K^+, as reported for both natural and synthetic zeolites (Guaya et al., 2015; Wu et al., 2006). Phosphate and potassium sorption kinetics are comparable with ammonium exchange kinetics, although more complex mechanisms are involved (e.g., complexation and precipitation of phosphates with calcium and/or potassium ions, and with the ≅AlOH and ≅FeOH surface groups and Ca(II) ions on CaP1). In fact, Ca^{2+}/NH_4^+ exchange on CaP1 in mixed Feed water with PRS is the driving force for the formation of calcium phosphate, followed by reaction of the free Ca^{2+} ions with phosphate ions

when saturation is reached (Watanabe et al., 2014). Under these conditions, in terms of the concentration of N, P, and K, and as shown for the co-precipitation of magnesium potassium phosphate (MPP: $MgKPO_4 \cdot 6H_2O$) and magnesium ammonium phosphate (MAP: $MgNH_4PO_4 \cdot 6H_2O$), the N-P-K exchange/sorption processes is described below.

a) NH_4^+ and K^+ cations exchanged with the Na^+ and Ca^{+2} ions from NaP1 and CaP1 as per Eq. 3:

$$ZO^- M^{n+} + nNH_4^+ / K^+ \leftrightarrow nZO^- NH_4^+ / K^+ + M^{n+} \quad \text{where } M^{n+} = Na^+ \text{ or } Ca^{2+} \tag{3}$$

where $\cong ZO^-$ represents the anionic groups of the zeolite structure, M^{n+} represents the exchangeable ions in the zeolite, and n is the cation charge.

b) Phosphate removal by formation of Ca-phosphates with the Ca^{2+} ions from the zeolite ion-exchange groups, as described by Eq. 4:

$$(\cong ZO^-)_2\ Ca^{2+} + H_2PO_4^- + 2Na^+ \leftrightarrow 2 \cong (ZO^-Na^+) + CaHPO_4\ (s) + H^+ \tag{4}$$

c) Ammonium, phosphate, and potassium removal with caustic magnesia (MgO) is expected through the formation of MAP or MPP, as described by Eqs. 5 and 6 (Ariyanto et al., 2013; Wilsenach et al., 2007):

$$Mg^{2+} + NH_4^+ + HPO_4^{-2} + 6H_2O \rightarrow MgNH_4PO_4 \cdot 6H_2O\ (s) + H^+ \tag{5}$$

$$K^+ + Mg^{2+} + HPO_4^{-2} \rightarrow KMgPO_4\ (s) + H^+ \tag{6}$$

3.3 Evaluation of the hybrid sorption/UF system for simultaneous N-P-K removal using PRS mixtures (NaP1/CaP1/MgO)

3.3.1 Performance of the hybrid sorption-membrane UF system using synthetic sludge anaerobic digestion side-stream feeds and CaP1/NaP1 mixtures (UF_A)

The N-P-K sorption capacity and removal efficiency using a mixture of NaP1 and CaP1 (UF_A) at constant pH (8.1±0.5) as a function of time are shown in Figure 3. The removal efficiency remained constant during the filtration cycle, returning values of 78±5, 32±3, and 26±3% with a maximum

253 sorption capacity of 35±3, 210±9, and 8±2 mg/g PRS for phosphate, ammonium, and potassium,

254 respectively.

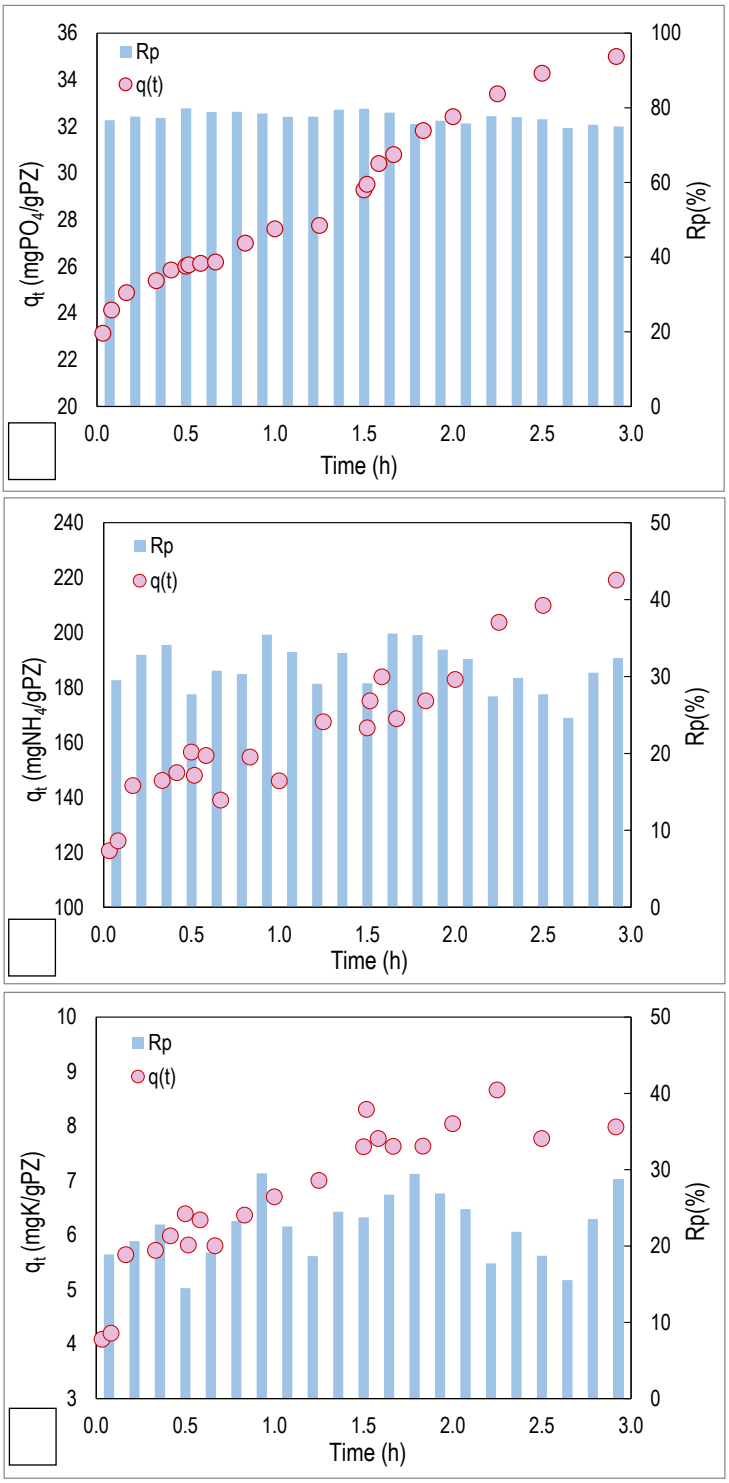

255

Figure 3. a) Phosphate, b) ammonium, and c) potassium recovery percentage (%) and sorption capacity q_t as a function of time for mixtures of NaP1 and CaP1 (UF_A) using synthetic sewage sludge anaerobic side-streams as feed solutions.

The N-P-K loading values (q_t) during the filtration cycles (Figure 3) increased over time with a maximum recovery for ammonium of 210±9 mg/g PRS and, by the end of the filtration test, the PRS had not reached saturation yet. However, this value was higher compared to the maximum ammonium sorption capacities reported by NaP1 and CaP1 in isotherm experiments, it can suggests that the precipitation of struvite is one the main mechanism on ammonium removal and plays a significant role in overall performance of hybrid sorption/filtration system.

The concentration ratios (C_t/C_0) of ammonium, phosphate, and potassium in the reactor reached values of 0.6±0.05, 0.2±0.04, and 0.8±0.04, respectively, as shown in Figure S1 (Supplementary Information).

The concentration ratios (C_t/C_0) of anions and cations in the STR effluent (T) and the feed stream (S) during the experiments are presented in Figure S1. The C_t/C_0 ratio for calcium decreased to 0.83±0.05, indicating the precipitation of Ca-phosphates and upon exchange with the free sites of CaP1 zeolite. Moreover, the sodium concentration decreased to 0.8±0.05 to compensate the exchanged positions on NaP1/CaP1 due to K^+ and NH_4^+ extraction, as expected, due to the high affinity of the zeolites for NH_4^+ and K^+. A 10% reduction of the magnesium concentration at the end of the experiment was observed. Scanning Electron Micrscopy with Energy Dispersive X-Ray (SEM-EDAX) analysis of the sorbent mixture at the end of the experiments revealed an increase of the Ca and K content with the decreasing Na content. Rich Ca and P mineral phases were detected on the zeolite structure; however, no Ca/Mg/K-phosphate phases were detected at ambient temperature by XRD analysis of the powder mixture after the UF_A experiments. Only the presence of calcium

aluminium phosphate $Ca_9Al(PO_4)_7$ was observed after thermal treatment at 1050 °C, as shown in Figure S2 (Supplementary Information).

3.3.2 Performance of the hybrid sorption-membrane UF system using synthetic sludge anaerobic digestion side-stream feeds and CaP1/NaP1/MgO mixtures (UF_B)

The N-P-K sorption capacity and removal efficiency as a function of the filtration time are shown in Figure 4. The pH was maintained constant at 8.2±0.3 and shorter filtration cycles were performed as the hydraulic operation limits of the UF module (2.5 g PRS/L) were approached, which required more back-washes. The removal efficiency for N-P-K remained constant during the experiment, while the sorption capacity (q_t) increased. The removal efficiency reached values of 20±2%, 85±5%, and 55±4, while the maximum sorption capacities (q_e) were 185±8, 32±3, and 23±2 mg/g PRS for ammonium, phosphate, and potassium, respectively.

The C_t/C_0 ratios for ammonium and phosphate in the reactor reached values of 0.8±0.05 and 0.2±0.05, respectively (Figure S3, Supplementary Information). The use of a tertiary mixture of sorbents did not afford any significant improvement of the system performance since the ammonium removal was slightly lower, while the phosphate removal efficiency was similar to that obtained with the binary mixture. The calcium concentration decreased considerably: according to Figure S3a, the C_t/C_0 ratio for calcium reached values of 0.35±0.05 due to the higher adsorption of Ca(II) by the zeolites and the precipitation of calcium phosphate, as described in Eq. 4. Moreover, the effect of calcium as a competitive cation was found to influence the adsorption of ammonium.

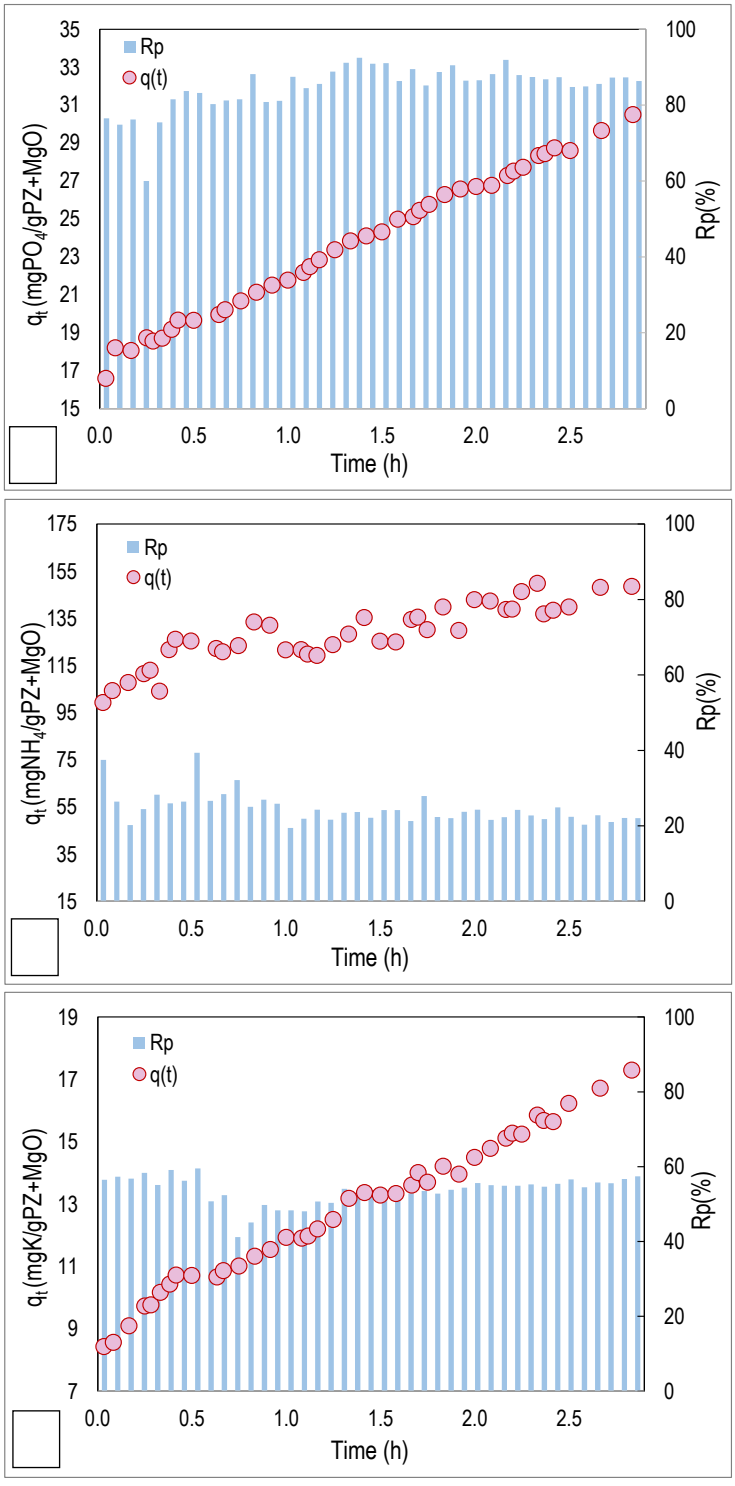

299

300 Figure 4. a) Phosphate, b) ammonium, and c) potassium recovery percentage (%) and sorption
301 capacity q_t as a function of time for mixtures of NaP1/CaP1/MgO (UF_B) using synthetic sewage
302 sludge anaerobic side-streams as feed solutions.

303 The sodium concentration remained constant during the cycles, and the same behaviour was
304 observed for the binary mixture (UF_A), suggesting that the exchange between ammonium and sodium
305 was not affected upon addition of MgO. The potassium concentration in this case decreased more
306 than with the UF_A mixture and the C_t/C_0 ratio reached values of 0.4±0.05, which could be the result of
307 removal through MPP precipitation, as described by Wilsenach et al., 2007, and Eq. 7 (Wilsenach et
308 al., 2007). SEM-EDAX analysis of the sorbent mixture at the end of the experiment revealed an
309 increase of the Ca, K, and Mg content and a reduction of the Na content. Rich Ca/P/O and Mg/P/N/O
310 mineral phases were detected on the zeolite structure; however, no Ca/Mg/K-phosphate phases were
311 detected.
312
313 3.3.3 Performance of the hybrid sorption-membrane UF system using sewage sludge anaerobic
314 digestion side-stream feeds and CaP1/NaP1 mixtures (UF_C)
315 The removal efficiency remained constant throughout the filtration cycle, returning values of 15±3,
316 65±5, and 6±2% for ammonium, phosphate, and potassium, respectively (Figure 5). Moreover, the
317 sorption capacity reached maximum values of 75±3, 52±3, and 5±1 mg/g PRS for each of those
318 species, respectively. The phosphate and ammonium loading values (q_t) during the filtration cycle
319 (Figure 5) increased over time, although the PRSs were not saturated at the end of the experiment.

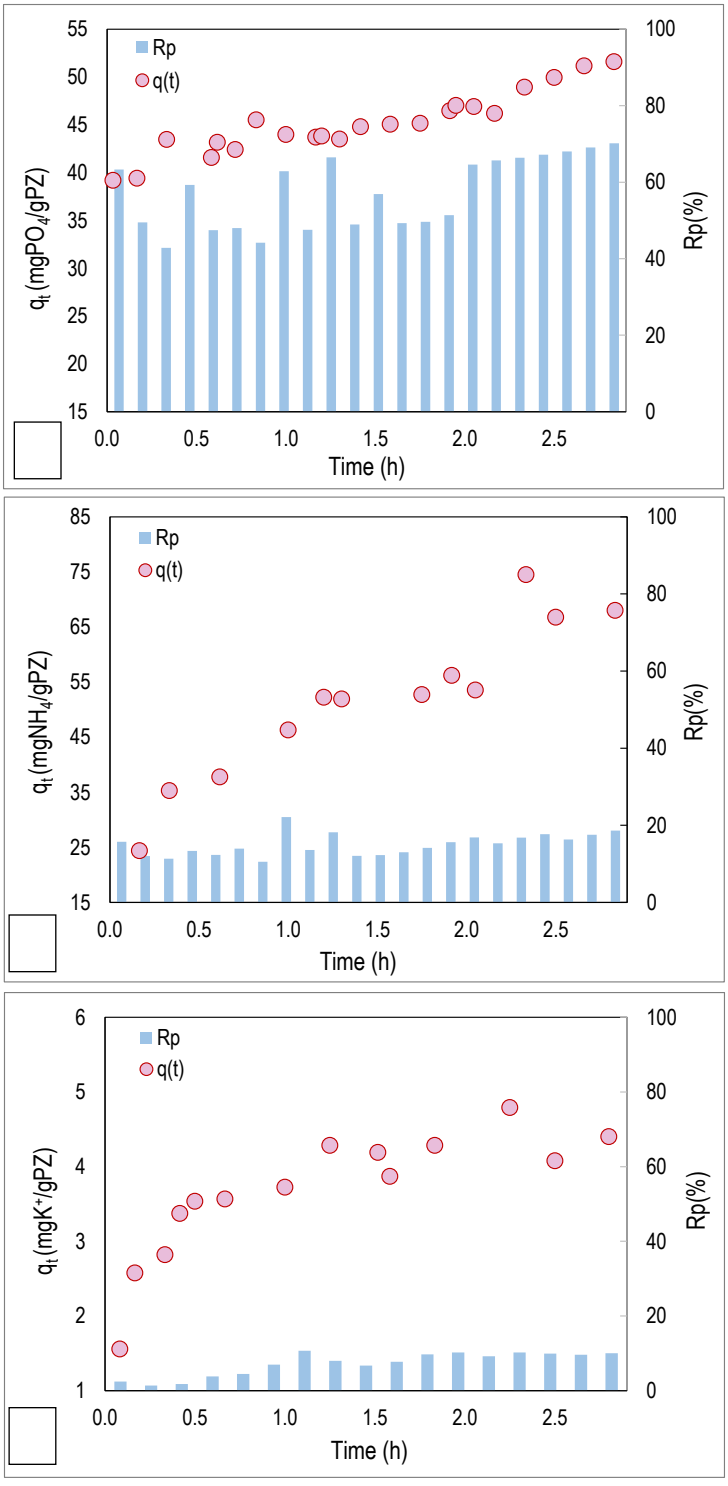

320

321 Figure 5. a) Phosphate, b) ammonium, and c) potassium recovery percentage (%) and sorption
322 capacity q_t as a function of time for mixtures of NaP1 and CaP1 (UF_c) using sewage sludge anaerobic
323 side-streams as feed solutions.

The sorbed P and N ratios in the reactor were below 1 during the filtration cycles, 0.2±0.05 and 0.7± 0.05 for phosphate and ammonium, respectively (Figure S4, Supplementary Information). Additionally, the C_t/C_0 ratios for potassium, calcium, magnesium, and sodium ranged between 0.8 and 0.9. As indicated by Eq. 4, the anionic groups of the zeolite structure must be neutralised upon consumption of Ca (II) during Ca-phosphate formation. Then, the cations in solution are exchanged according to the selectivity factors for $Na^+/Ca^{2+}/Mg^{2+}$ (Roberto T. Pabalan, 2001).

SEM-EDAX analysis of the sorbent mixture at the end of the experiment revealed an increase of the Ca and K content and a reduced Na content. Rich Ca and P mineral phases were detected on the zeolite structure; however, no Ca/K-Mg-phosphate phases were detected at ambient temperature by XRD analysis of the powdered mixture after the UF_c experiment, although N/Mg/P struvite was detected, as shown in Figure S5 (Supplementary Information). The average chemical composition of the three loaded PRS mixtures, as well as for the two virgin zeolites (NaP1 and CaP1), are summarised in Table 3.

Table 3. Average chemical composition (w/w) of the loaded zeolites mixtures and virgin PRS mixtures

Average / Experiments	O	Na	Mg	Al	Si	P	K	Ca	Fe
NaP1 (%)	50.6	7.6	0.5	8.1	15.1	0.2	1.8	1.4	2.9
CaP1 (%)	51.3	1.0	0.6	8.1	14.6	0.2	1.3	7.4	2.4
UF_A (%)	51.8	0.8	0.9	12.4	15.4	0.9	0.4	5.5	2.9
UF_B (%)	40.8	0.7	2.5	16.3	15.3	1.4	0.6	6.7	3.4
UF_C (%)	50.5	0.4	0.8	16.4	16.8	0.6	0.8	1.4	2.9

340 The sorption processes were accordingly correlated to changes on the main species involved (N, P,
341 K, Na, Ca, Mg). The highest content of phosphate was found in $UF_{B,}$ while the lowest content
342 corresponded to $UF_{C.}$ The highest potassium content was measured for the UF_C sample. The
343 nitrogen content could not me determined precisely due to the weak signal obtained from such a light
344 element.
345
346 **3.4. Hydraulic performance of the hybrid sorption/UF system**
347 The evolution of the TMP as the sorption/filtration experiments progressed is shown in Figure 6. The
348 TMP values increased with time, from an initial value of approximately 0.3 to a threshold value of 0.8
349 bar, at which point the filtration cycle was considered finished and a cleaning protocol was applied
350 (BW). Longer filtration cycles were carried out for the experiments with binary mixtures (UF_A with
351 synthetic feed and UFc) for comparison with the experiments with the tertiary mixture containing
352 MgO.

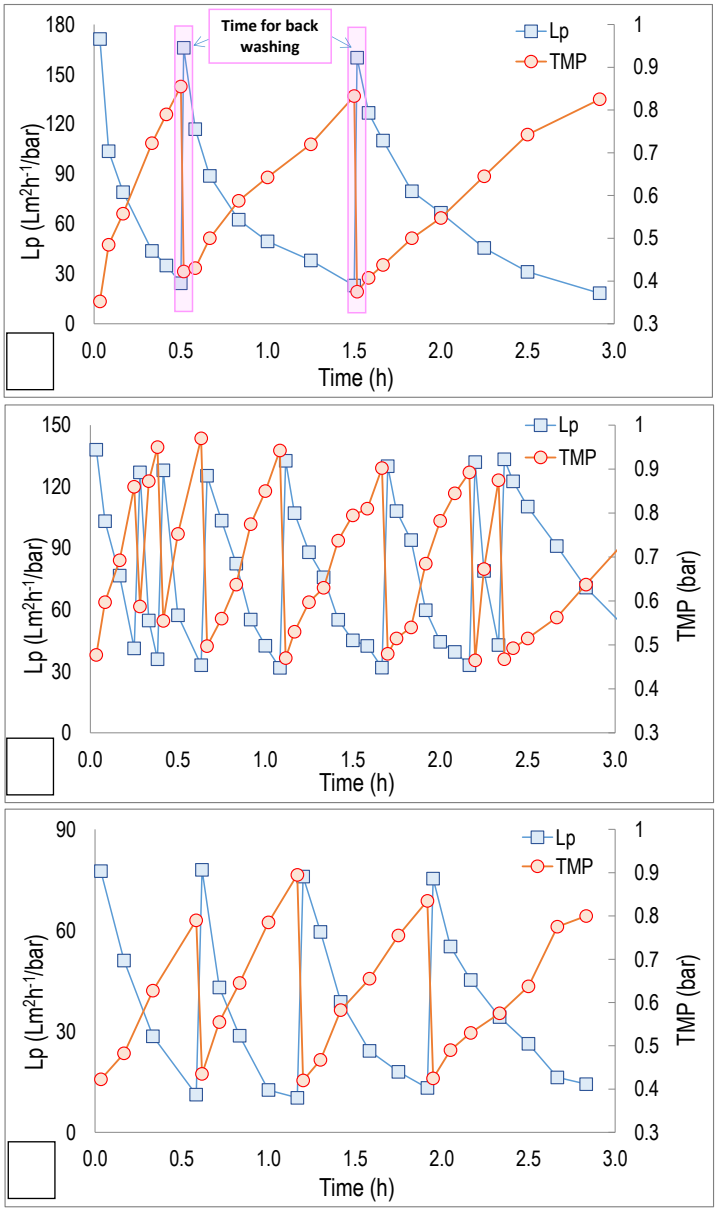

Figure 6. Variation of the transmembrane pressure (TMP) and the permeability (Lp, Lm^2h^{-1}/bar) with the time or the continuous sorption/UF system with a) UF_A: a) binary PRS mixture; b) UF_B: a tertiary PRS mixture, and c) UF_C: a binary PRS mixture.

The presence of caustic magnesia used in the form of very fine MgO particles obtained as a powder by-product from the air calcination of magnesium carbonate, affording incompressible cake layers. After the cleaning procedure (BW), the initial membrane permeability was recovered (170±10 and 138±8 Lm^2h^{-1}/bar for UF_A and UF_B, respectively), although a reduction in the permeability recovery

was observed in the experiments with the tertiary mixture and, in particular, the minimum value was recorded for UF_C (79±4 $Lm^{-2}h^{-1}bar^{-1}$), which was associated with the presence of colloidal material and a high concentration of initial total organic carbon (TOC = 299±10 mg/L). Yamini et al., 2009 (Satyawali and Balakrishnan, 2009), associated the decreases in permeability and changes in filtration processes with the particle size, since this affects the characteristics of the cake formed from the rejected solids. In fact, as mentioned in the experimental section, no chemicals were used during the backwash and the reduction in the permeability can be explained by the formation of a PRS cake on the membrane surface. For sludge particle sizes smaller than or comparable to those of the added PRSs with or without MgO, the final particle size could increase, as explained Park et al., 1999 (for the case of powder activated carbon (PAC)) (Park et al., 1999). The particle size increase is typically attributed to the adsorption of dissolved and colloidal organics and also free bacteria cells on the PRS particles. (Satyawali and Balakrishnan, 2009).

3.5. Evaluation of nutrient speciation and bioavailability of loaded reactive sorbents

The phosphate and ammonium speciation results for the loaded PRS samples, represented as mg/g PRS, are shown in Figure 7. The P speciation confirmed that the HCl-P fraction associated with the presence of Ca-phosphate mineral species (Meis et al., 2012; Wang et al., 2012) or Mg-ammonium-phosphate (struvite) was 120 mg $P\text{-}PO_4$/L for the UF_A and UF_B samples and up to 370 mg $P\text{-}PO_4$/L for UF_C. Additionally, the easily exchangeable speciation (KCl-P) associated with the formation of labile complexes with Al and Fe metal oxides contributed with 41 to 53 mg $P\text{-}PO_4$/L for UF_B and UF_A and 118 mg $P\text{-}PO_4$/L for the UF_C sample. In the case of ammonium, the highest fraction of the three samples was associated with a labile exchange fraction, confirming that the main mechanism in both zeolites is ion-exchange. Only in the UF_C sample, where struvite was identified by XRD analysis, the fraction with HCl represented an important contribution (350±50 mg $N\text{-}NH_4$/L). The mixtures of

reactive sorbents, obtained as by-products of industrial waste (e.g., zeolites produced from fly ash or caustic magnesia from magnesium carbonate furnaces) afforded both good sorption properties and release ratios. Depending on the composition of the solution to be treated, the composition of the sorbent mixture should be tuned to optimise the nutrient release ratios.

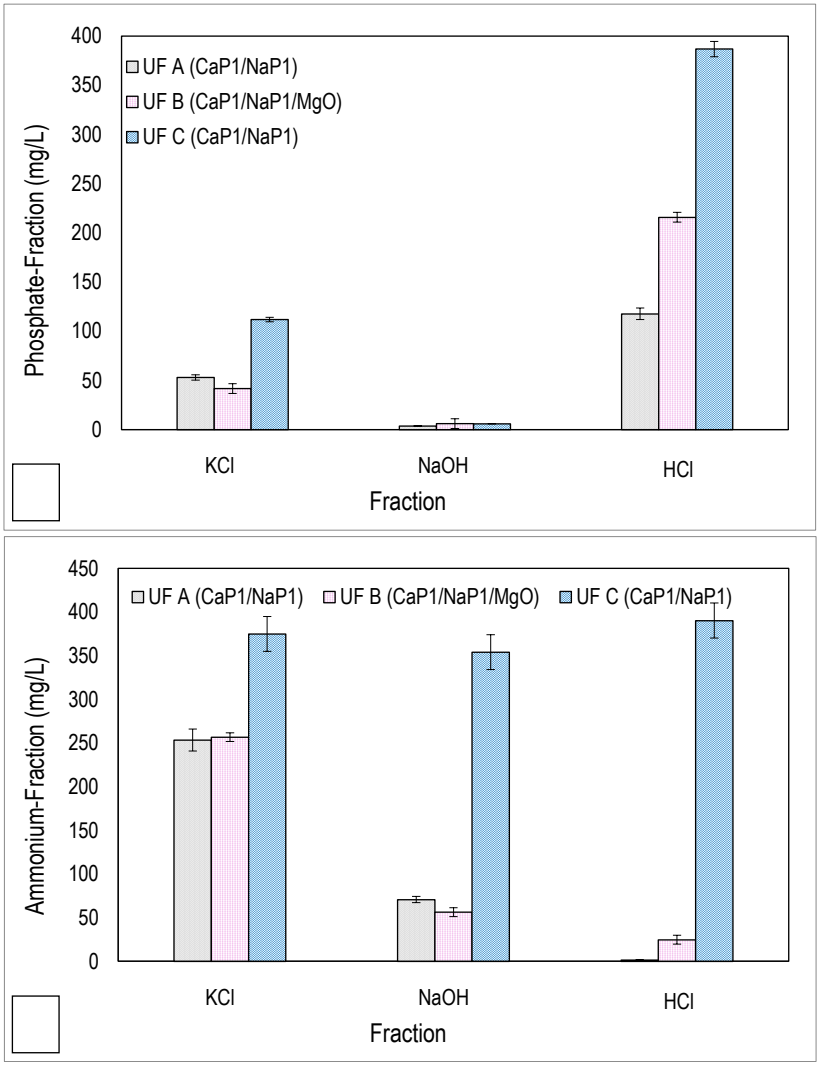

Figure 7. Speciation of the PRSs for the UF experiments: a) phosphate and b) ammonium fractions.

The determination of nutrient availability based on the Olsen method (Olsen., 1954) uses bicarbonate extraction as a suitable method for predicting the plant availability of phosphate species in calcareous soils, where the main role of $NaHCO_3$ in phosphate extraction is decreasing the Ca^{2+} activity by

395 forming $CaCO_3$. The phosphate-availability data for 0.5 M solutions of $NaHCO_3$ are plotted in Figure 8
396 as the extracted amount of phosphate per mass of loaded sorbent powder (mg $P\text{-}PO_4$/g). In the
397 presence of excess bicarbonate, the labile phosphate fraction (P-KCl) and partial brushite and
398 struvite dissolution occur according to Eq. 8 and 9:
399
400 $CaHPO_4(s) + HCO_3^- = CaCO_3(s) + H_2PO_4^-$ $\log K = -1.3$ (25 °C) (8)
401 $NH_4MgPO_4(s) + HCO_3^- = MgCO_3(s) + HPO_4^{-2} + NH_4^+$ $\log K = -3.1$ (25 °C) (9)
402
403 The potassium-availability data is presented as the extracted amount of phosphate per mass of
404 loaded sorbent powder (mg $P\text{-}PO_4$/g), which revealed similar ratios from 0.5 to 1.5 mg K/g for UF_C.
405 Moreover, the maximum ratio for ammonium was found to range from 12 to 18.5 mg NH_4^+/g for $UF_{A\text{-}B}$
406 and UF_C. These results are in good agreement for the presence of PRS in ammonium and potassium
407 form (NaP1/CaP1/N-K) as well as minerals as struvite.
408 The phosphate, potassium, and ammonium species sorbed on the PRSs samples were thus
409 demonstrated to dissolve in solutions containing moderate-to-high bicarbonate concentrations, similar
410 to those expected in basic soils characterised by high calcareous rock content (e.g., limestone) and
411 where other Ca/Mg-phosphate minerals, such as hydroxyapatite and struvite (MAP and MPP), are
412 very insoluble and thus offer limited plant availability.

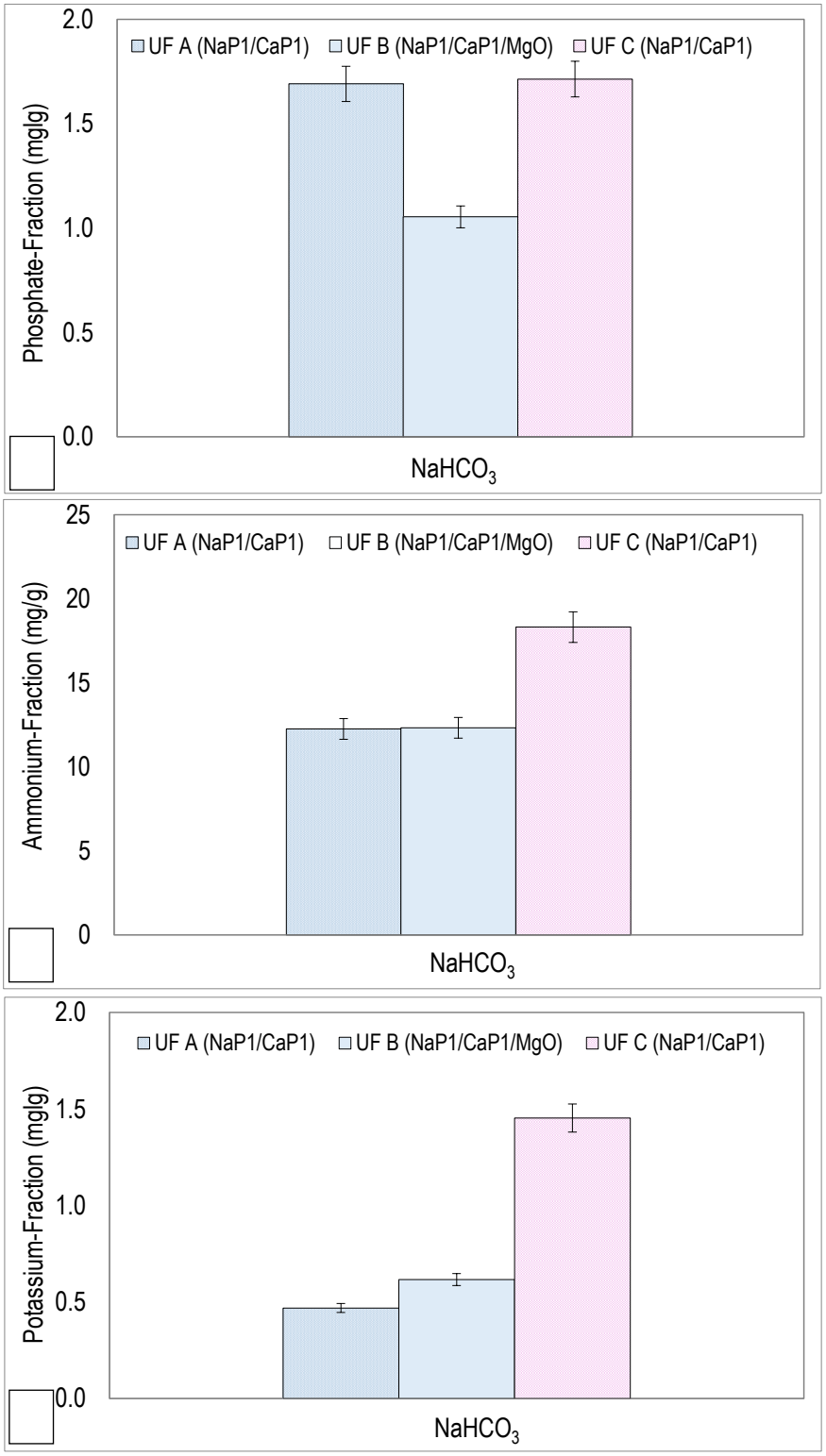

Figure 8. a) Phosphate, b) ammonium, and c) potassium extraction from loaded PRSs using $NaHCO_3$ solutions (0.5 M).

4. Conclusions

Mixtures of reactive sorbents (Na/CaP1 zeolites and a magnesium oxide-rich waste) were shown to be effective for the recovery of N-P-K from potassium-rich sewage sludge anaerobic digestion side-streams. Binary and tertiary mixtures showed that the sodium zeolite (NaP1) provided efficient removal of NH_4^+ and K^+, the Ca-zeolite (CaP1) facilitated the removal of phosphate by formation of Ca-phosphates (CaHPO4(s)), and caustic magnesia containing MgO facilitated the formation of $Mg/NH_4/PO_4$ minerals (e.g., struvite and magnesium phosphates). The continuous and simultaneous removal of ammonium, phosphate, and potassium ions with mixtures of powder reactive sorbents (2–2.5 g PRS/L) using a hybrid sorption/filtration system afforded removal capacities of 220±10 mg N-NH_4/g, 35±5 mg P-PO_4/g, and 8±2 mg K/g for binary mixtures of NaP1/CaP1. Contrary to the batch results, the use of tertiary mixtures of NaP1/CaP1/MgO only improved the K removal capacity, while the phosphate removal capacity was maintained and the NH_4^+ capacity was reduced due to the competence of Mg^{+2} ions in the ion-exchange sites. Nutrient removal trials with real anaerobic side-streams using binary mixtures of Na/CaP1 showed a decrease in both the hydraulic performance and the nutrient removal ratios due to the presence of dissolved organic matter. The sorption reaction mechanisms were also confirmed by structural and textural analyses. Chemical analyses confirmed the formation of Ca/P and Mg/N/P minerals; however, the presence of brushite and struvite was detected by mineralogical characterisation. The constant removal ratios of N, P, and K were measured in relation to the filtration time. The N-P-K-loaded sorbents showed good nutrient release and bioavailability ratios as co-substrates for soil quality improvement.

Acknowledgments

This study has been supported by the ZERODISCHARGE project (CTQ2011-26799) and the Waste2Product project (CTM2014-57302-R) financed by Ministry of Science and Innovation (MINECO, Spain) and the Catalan government (project ref. 2014SGR050). Pentair X-Flow is acknowledged for the supply of the UF module. R. Estany (Aigues de Barcelona) and M. Gullom (EMMA) and I. Sancho (Centro Tecnologíco del Agua (CETAQUA)) for waste water samples supply.

5. References

Ann, Y., Reddy, K.R., Delfino, J.J., 2000. Influence of chemical amendments on phosphorus immobilization in soils from a constructed wetland 14, 157–167.

Ariyanto, E., Kanti, T., Ming, H., 2013. The influence of various physico-chemical process parameters on kinetics and growth mechanism of struvite crystallisation. Adv. Powder Technol. 25, 682–694.

Bartzokas, A., 2003. Environmental regulation and corporate strategies in the fertiliser industry. Int. J. of Agricultural Resources, Governance and Ecology. 2, 262 - 294.

Dong, H., Gao, B., Yue, Q., Sun, S., Wang, Y., Li, Q., 2014. Floc properties and membrane fouling of different monomer and polymer Fe coagulants in coagulation–ultrafiltration process: The role of Fe (III) species. Chem. Eng. J. 258, 442–449.

European Commission, 2014. Review of the list of critical raw materials for the EU and the implementation of the Raw Materials Initiative. COM 10457/14 297, Brussels, Belgium, June 3rd.

Gray-Munro, J.E., Strong, M., 2013. A study on the interfacial chemistry of magnesium hydroxide surfaces in aqueous phosphate solutions: influence of Ca^{2+}, Cl^- and protein. J. Colloid Interface Sci. 393, 421–428.

464 Guaya, D., Valderrama, C., Farran, A., Armijos, C., Cortina, J.L., 2015. Simultaneous phosphate and
465 ammonium removal from aqueous solution by a hydrated aluminum oxide modified natural
466 zeolite. Chem. Eng. J. 271, 204–213.
467 Hermassi, M., Valderrama, C., Gibert, O., Moreno, N., Font, O., Querol, X., Batis, N., Cortina, J.L.,
468 2016a. Integration of powdered Ca-activated zeolites in a hybrid sorption-membrane
469 Ultrafiltration process (PAZ-UF) for phosphate recovery. Ind. Eng. Chem. Res. 55, 6204–6212.
470 Hermassi, M., Valderrama, C., Moreno, N., Font, O., Querol, X., Batis, N., Cortina, J.L., 2016b.
471 Powdered Ca-activated zeolite for phosphate removal from treated waste-water. J. Chem.
472 Technol. Biotechnol. 91, 1962‐1971.
473 Kumar, R., Pal, P., 2013. Turning hazardous waste into value-added products: Production and
474 characterization of struvite from ammoniacal waste with new approaches. J. Clean. Prod. 43,
475 59–70.
476 Lalley, J., Han, C., Li, X., Dionysiou, D.D., Nadagouda, M.N., 2016. Phosphate adsorption using
477 modified iron oxide-based sorbents in lake water: Kinetics, equilibrium, and column tests.
478 Chem. Eng. J. 284, 1386–1396.
479 Ledda, C., Schievano, A., Salati, S., Adani, F., 2013. Nitrogen and water recovery from animal
480 slurries by a new integrated ultrafiltration, reverse osmosis and cold stripping process: A case
481 study. Water Res. 47, 6157–6166.
482 Hedley, M.J., Stewart, J.W. B., Chauhan, B.S., 1982. Changes in Inorganic and Organic Soil
483 Phosphorus Fractions Induced by Cultivation Practices and by Laboratory Incubations.
484 Soil.Sci.AM.J 46, 970–976.
485 Masse, L., Masse, D.I., Pellerin, Y., 2007. The use of membranes for the treatment of manure : a
486 critical literature review. Biosyst. Eng. 98, 371–380.

487 Meis, S., Spears, B.M., Maberly, S.C., O'Malley, M.B., Perkins, R.G., 2012. Sediment amendment
488 with Phoslock® in Clatto Reservoir (Dundee, UK): Investigating changes in sediment elemental
489 composition and phosphorus fractionation. J. Environ. Manage. 93, 185–193.
490 Moharami, S., Jalali, M., 2014. Phosphorus leaching from a sandy soil in the presence of modified
491 and un-modified adsorbents. Environ. Monit. Assess. 186, 6565–76.
492 Olsen, S.R. ; Cole, C.V; Watanabe, F.S; Dean, L.A, 1954. Estimation Of Available Phosphorus In
493 Soils By Extraction With Sodium Bicarbonate, United Sta. ed. United States Department Of
494 Agriculture ; Washington, DC .USDA Circ. 939.
495 Onyango, M.S., Kuchar, D., Kubota, M., Matsuda, H., 2007. Adsorptive removal of phosphate ions
496 from aqueous solution using synthetic zeolite. Ind. Eng. Chem. Res. 46, 894–900.
497 Park, H., Choo, K.-H., Lee, C.-H., 1999. Flux Enhancement with Powdered Activated Carbon Addition
498 in the Membrane Anaerobic Bioreactor. Sep. Sci. Technol. 34, 2781–2792.
499 Petersen, S.O.,et al., 2007. Recycling of livestock manure in a whole-farm perspective. Livest. Sci.
500 112, 180–191.
501 Puidomènech, I.S.S., 2001. Chemical Equilibrium Software Hydra and Medusa. Stock. Sweden.
502 Querol, X., Moreno, N., Alastuey, A., Juan, R., Ayora, C., Medinaceli, A., Valero, A., Productos, C.,
503 2007. Synthesis of high ion exchange zeolites from coal fly ash. Geol. Acta 5, 49–57.
504 Roberto T. Pabalan, F.P.B., 2001. Cation-exchange properties of natural zeolites. Rev. Mineral.
505 geochemistry . Nat. zeolites Ocurr. proerties, Appl. Eds. Bish.
506 Satyawali, Y., Balakrishnan, M., 2009. Effect of PAC addition on sludge properties in an MBR treating
507 high strength wastewater. Water Res. 43, 1577–1588.
508 Schoumans, O.F., Bouraoui, F., Kabbe, C., Oenema, O., van Dijk, K.C., 2015. Phosphorus
509 management in Europe in a changing world. Ambio 44, 180–192.
510 Taddeo, R., Kolppo, K., Lepist, R., 2016. Sustainable nutrients recovery and recycling by optimizing

511 the chemical addition sequence for struvite precipitation from raw swine slurries 180, 52–58.
512 Van Kauwenbergh, S.J., Stewart, M., Mikkelsen, R., 2013. World Reserves of Phosphate Rock-a
513 Dynamic and Unfolding Story. Better Crop. 97, 18–20.
514 Wang, C., Qi, Y., Pei, Y., 2012. Laboratory investigation of phosphorus immobilization in lake
515 sediments using water treatment residuals. Chem. Eng. J. 209, 379–385.
516 Wang, H., Qu, F., Ding, A., Liang, H., Jia, R., Li, K., Bai, L., Chang, H., 2016. Combined effects of
517 PAC adsorption and in situ chlorination on membrane fouling in a pilot-scale coagulation and
518 ultrafiltration process. Chem. Eng. J. 283, 1374–1383.
519 Watanabe, Y., Yamada, H., Ikoma, T., Tanaka, J., Stevens, G.W., Komatsu, Y., 2014. Preparation of
520 a zeolite NaP1/hydroxyapatite nanocomposite and study of its behavior as inorganic fertilizer. J.
521 Chem. Technol. Biotechnol. 89, 963–968.
522 Wilsenach, J.A., Schuurbiers, C.A.H., van Loosdrecht, M.C.M., 2007. Phosphate and potassium
523 recovery from source separated urine through struvite precipitation. Water Res. 41, 458–466.
524 Wu, D., Zhang, B., Li, C., Zhang, Z., Kong, H., 2006. Simultaneous removal of ammonium and
525 phosphate by zeolite synthesized from fly ash as influenced by salt treatment. J. Colloid
526 Interface Sci. 304, 300–306.
527 Xu, K., Li, J., Zheng, M., Zhang, C., Xie, T., Wang, C., 2015. The precipitation of magnesium
528 potassium phosphate hexahydrate for P and K recovery from synthetic urine. Water Res. 80,
529 71–79.
530 You, X., Valderrama, C., Cortina, J.L., 2017. Simultaneous recovery of ammonium and phosphate
531 from simulated treated wastewater effluents by activated calcium and magnesium zeolites.
532 Chem. Technol. Biotechnol. doi:DOI: 10.1002/jctb.5249
533 Zhang, B.-H., Wu, D.-Y., Wang, C., He, S.-B., Zhang, Z.-J., Kong, H.-N., 2007. Simultaneous removal
534 of ammonium and phosphate by zeolite synthesized from coal fly ash as influenced by acid

treatment. J. Environ. Sci. (China) 19, 540–5.